

PREPARATION OF CZTS DEPOSITS ON GOLD SUBSTRATE BY ELECTROCHEMICAL DEPOSITION- ANNEALING EFFECT

A. PARAYE, R. MANIVANNAN, S. N.VICTORIA SELVAM*

Department of Chemical Engineering, National Institute of Technology Raipur, Raipur 492010, INDIA

Room temperature one-step electrodeposition of chalcogenide CZTS followed by annealing at different temperatures was studied. The scanning electron microscopy images of the deposits confirmed the presence of agglomerated particles in the deposits. The deposits annealed at 400°C did not show the presence of voids whereas deposits annealed at 500°C showed severe sulfur loss and were off-stoichiometric. Annealing at 400°C resulted in the deposits of compositions closer to the required ratio. Good absorbance over the entire visible range makes both the annealed deposits suitable absorber materials for thin-film photovoltaic cells. Current-voltage characteristics resulted in Ohmic trend and the slope of the plot increased with annealing temperature. The deposits showed good photosensitive behavior where resistance decreased upon shining the light source. The Mott-Schottky plot showed that the deposits were made of positively charged particles.

(Received October 16, 2019; Accepted February 18, 2020)

Keywords: Chalcogenide, Absorber material, CZTS, Annealing temperature, Electrochemical deposition

1. Introduction

Growing population and technological advancements have increased the day to day energy requirement drastically. To address this ever-increasing energy scarcity, the utilization of solar energy has gained importance which in turn increased the demand for suitable solar cells. Silicon thin-film photovoltaic cells are expensive and require thicker absorber because of the indirect band gap of silicon [1, 2]. A suitable replacement for silicon is chalcogenide copper zinc tin sulfide (CZTS), which is a direct band gap semiconductor and has a higher coefficient of absorption for light ($> 10^4 \text{ cm}^{-1}$) than silicon resulting in the requirement of thin absorber layer [3]. The raw materials for CZTS are also available in plenty and are also environmental friendly.

CZTS thin films are usually prepared using more energy-consuming routes such as chemical vapor deposition, sputtering, spray pyrolysis, thermal evaporation and electron beam evaporation [4] which involves deposition either at high temperature or vacuum. There are some simple techniques that enable CZTS deposition at low temperature and atmospheric pressure conditions. These include electrochemical deposition, successive ionic layer adsorption and reaction, spin coating and chemical bath deposition [5, 6]. Out of these, electrochemical deposition is highly preferred owing to the advantages including easy scalability and better control over the process [7]. Both water and ionic liquids have been studied as a solvent for the CZTS electrodeposition [7-13]. Ethylene glycol and choline chloride were used as a solvent in a study for the electrodeposition of CZTS [8]. In the first step copper, zinc and tin were co-electrodeposited and sulfur was included during annealing in the second step [8]. Most of the literature on the electrochemical deposition of CZTS use sequential multistep deposition of the elements on to a substrate followed by sulfurization at low or moderate to high temperatures [7, 8, 11]. Such multistep deposition processes require more reaction time and there is a need to confirm that the former layer adheres well so that the subsequent layer can be deposited [14]. Sulfurization at high temperatures was found to cause cracks and affect the strength of the film [10]. To avoid such issues, it is preferred to include sulfur during the electrochemical deposition step. More preferred is the electrodeposition of all the four elements in a single-step.

* Corresponding author: snvictoria.che@nitrr.ac.in

However, depositing of all the four elements in a single-step requires careful selection of a suitable complexing agent to bring the deposition potentials of copper, zinc, tin and sulfur closer so that all the four elements can be electrodeposited at a single reduction potential. The complexing agent extensively studied for such electrodeposition of CZTS is a combination of trisodium citrate and tartaric acid [7, 12, 15, 16]. The use of sodium thiocyanate for CZTS electrodeposition in a single-step on an ITO substrate has been reported [9, 10]. Recently our group has reported the use of glycine for successful electrochemical deposition of CZTS in one-step [2]. The work concluded that the properties of the deposits prepared are significantly altered by the factors in order $\text{pH} > \text{annealing temperature} > \text{S precursor concentration}$ [2]. This work discusses in detail the properties of the CZTS deposits prepared by the electrodeposition process using glycine and subsequent annealing at two different temperatures.

2. Materials and methods

The concentration of the precursor chemical and the procedure for electrochemical deposition of CZTS have been discussed in detail elsewhere [2]. In brief, sulfates of copper and zinc were used as Cu (10 mM) and Zn (20 mM) precursors while stannous chloride was used as the Sn (5 mM) source. Sodium thiosulfate was used as the S (80 mM) source and glycine as the complexing agent. The medium pH was maintained at 2.5. The CZTS film was deposited on a gold substrate. The deposition potential used for the study was -0.86 V and the potentiostatic deposition was continued for 20 min.

2.1. Characterization studies

The CZTS film thus obtained after 20 min was annealed at 400°C and 500°C for 30 min in Ar medium. The effects of annealing on crystalline nature, morphology and optical band gap were investigated using X-ray diffraction, scanning electron microscopy, UV-vis spectroscopy respectively. I-V characterization was carried out for the sandwich of gold and CZTS in the light and dark using 200 W light source. The Mott Schottky runs were made using the CZTS coated gold slide working electrode and the electrolyte was 0.1 M sodium perchlorate. The Mott-Schottky measurements were made at 1000 Hz frequency.

3. Results and discussion

3.1. Scanning electron microscopy (SEM)

The surface images of the electrodeposited films after annealing at 400°C and 500°C for 30 min are shown in Figs. 1a and b respectively. From Fig. 1a, it is clear that annealing at 400°C produced agglomerated particles in the film. However, the majority of the film is found to be composed of uniformly sized smaller less dense agglomerates. The formation of agglomerates is preferred for absorber layer in thin-film photovoltaic cells because of decreased chances of recombination of the charge carriers [16]. The deposit obtained after annealing at 500°C (Fig. 1b) shows the presence of many larger aggregates and voids which could be due to the liberation of volatile S and Sn compounds [17]. Similar behavior was observed when CZTS prepared by solvothermal route was annealed at temperatures from 200°C to 400°C. Sulfur content dropped significantly and metals to sulfur ratio increased from 0.8 at 300°C to 1.07 at 400°C [18].

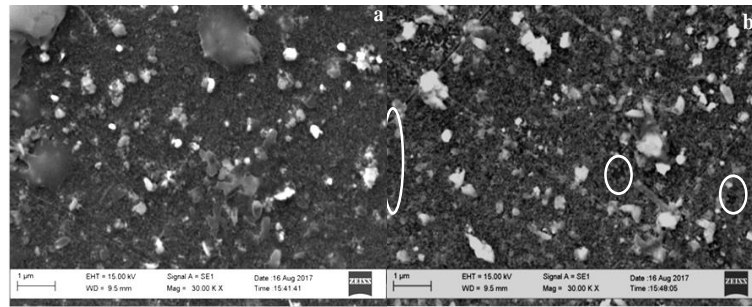


Fig. 1. SEM images of annealed CZTS thin films (a). 400°C (b). 500°C.

The elemental compositions of the annealed CZTS deposits can be obtained from Table 1. The samples annealed at 400°C show a desirable composition ratio of 2:1:1:4 for Cu, Zn, Sn, and S respectively. Moreover, from Table 1 the ratio of Cu composition to (Zn+Sn) composition is 0.85 and Zn to Sn composition is 0.88 which makes the film copper poor and slightly tin rich. Annealing at 500°C caused significant changes in the stoichiometry resulting in an off-stoichiometric deposit. The SEM images show the existence of voids in the samples annealed at 500°C, while the annealing process at 400°C did not cause any void formation. The formation of volatile S can be confirmed with the drop in the S content of the sample heated at 500°C. The composition ratio of all the metallic elements to the sulfur content increased from 1.8 to 2.5 when the annealing temperature was increased from 400°C to 500°C respectively.

Table 1 Atomic percentage of the elements in the annealed CZTS deposits.

Elements	400°C	500°C
Cu	26.81	27.93
Zn	14.78	13.20
Sn	16.77	29.96
S	41.65	28.91
[Zn]/[Sn]	0.88	0.44
[Cu]/[Zn]+[Sn]	0.85	0.65

3.2. X-ray diffraction

The results of X-ray diffraction analysis for the annealed CZTS deposits are shown in Fig. 2. The peaks that correspond to the CZTS are of low intensity for both the deposits indicating the amorphous nature of the deposits. The hump at 23.14° observed in both samples represents the (110) plane of the kesterite phase CZTS. Similarly, peaks at 28.74°, 44.93° and 47.76° correspond to (112), (123) and (220) planes of kesterite phase CZTS respectively. Secondary phases such as Cu₄SnS₄ were also observed [9,10,19]. With an increase in annealing temperature the secondary phase growth enhanced while the peak at 28.7° corresponding to (112) plane of kesterite structure disappeared. The development of secondary phases has been related to high-temperature annealing or increased annealing time [1, 19].

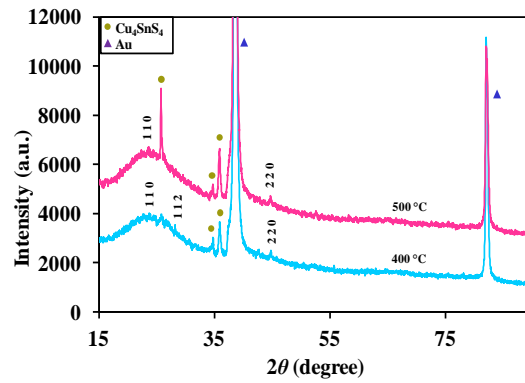


Fig. 2. XRD spectra recorded for the annealed CZTS deposits prepared by electrodeposition.

3.3 UV-vis spectroscopy

The absorbance spectra for the electrodeposited CZTS films after annealing are presented in Fig. 3. Both films show higher absorbance over a broad wavelength range including visible and IR regions. The absorbance spectra match well with the earlier reports [16]. A material showing high absorbance in the visible region is ideal for photovoltaic applications. The optical band gap value for the annealed thin films can be found out from Tauc's relation that describes the absorption coefficient (α) in terms of photon energy (E) as shown in 1.

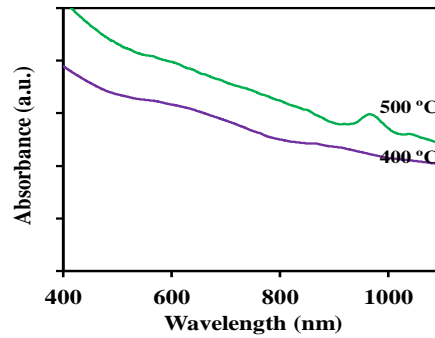


Fig. 3. Absorbance spectra of the CZTS deposits.

$$(\alpha E)^{\frac{1}{n}} = A^{\frac{1}{n}}(E - E_g) \quad (1)$$

The constant n is assigned a value $\frac{1}{2}$ for direct-allowed band gap materials, $\frac{3}{2}$ for the indirect-forbidden band gap materials and 3 for indirect-allowed band gap materials [2, 3]. A plot between $(\alpha E)^{1/n}$ and E , then would provide details of the band gap value (E_g) upon extending the straight-line segment to zero absorption coefficient. The n value for CZTS is $\frac{1}{2}$ since it is a direct band gap material. Fig. 4 shows the Tauc plots of the annealed CZTS deposits. It can be inferred that the deposits have an absorption coefficient greater than 10^4 which is highly preferred for the photovoltaic applications. The optical band gap value for both films is nearly the same which is equal to 1.6 eV. The band gap for the CZTS reported from the previous works varies between 1.45 and 1.7 eV with the composition and secondary phases present [16]. The value obtained in the present study matches well with the earlier reports.

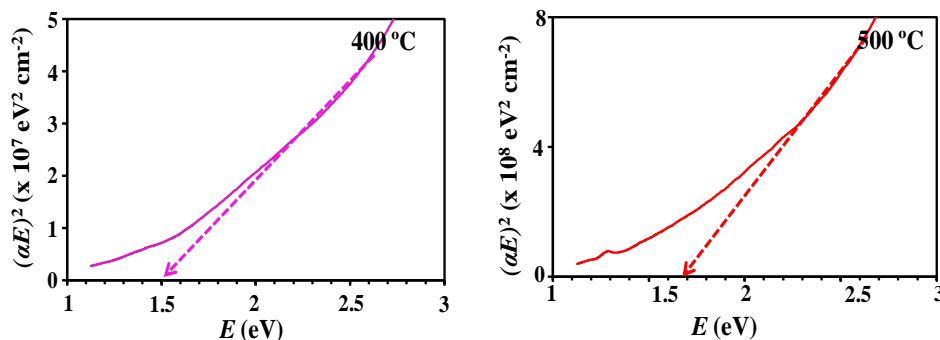


Fig. 4. Tauc plot for thin film annealed at different temperatures.

3.4. Current- potential studies

The current-potential behavior for the sandwich formed using annealed CZTS deposits are shown in Fig. 5. The patterns present a straight-line behavior displaying Ohmic nature. The slope of the straight lines gives the value of resistance. The resistance values for the CZTS films annealed at 400°C and 500°C in the absence of light are 33 Ω and 100 Ω respectively. In the light mode, the resistance value decreased significantly to 20 Ω and 30 Ω for the samples annealed at 400 °C and 500 °C respectively. The resistance values match well with the earlier reports on the current potential characteristics of CZTS [11]. A drop in the resistance in light is attributed to the electron-hole pairs formed in the conduction and valence bands due to the incident photon [20].

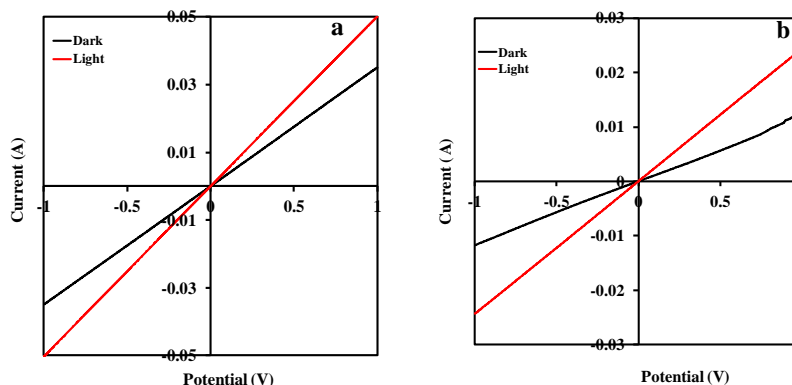


Fig. 5. I-V plots for the annealed CZTS deposits in dark and light (a) 400°C, (b) 500°C

3.5. Capacitance-potential study

The majority charge carriers in CZTS chalcogenides are holes and thus make them p-type. The conductivity of the electrodeposited CZTS deposits after annealing was studied by capacitance-voltage characteristics at a constant frequency. The resulting Mott-Schottky diagrams are plotted for the films and are shown in Fig. 6. A negative slope for the straight-line portion in the Mott-Schottky plot indicates p-type conductivity with charge carriers as holes. A positive slope shows the n-type conductivity with electrons as the charge carriers [3]. The Mott-Schottky plots for the CZTS films annealed at 400°C and 500°C show a negative slope signifying the formation of p-type deposits upon annealing. The concentration of the charge carriers (N) can be calculated using the static relative dielectric constant for CZTS (ϵ), electron charge (e) in Coulombs and the permittivity of free space in the vacuum (ϵ') from the equation described elsewhere [3]. Using a value of 4.27 for ϵ , the charge carrier concentration for the CZTS annealed at 400°C and 500°C in order are $8.2 \times 10^{19} \text{ cm}^{-3}$ and $6.62 \times 10^{17} \text{ cm}^{-3}$.

For a semiconductor in contact with an electrolyte, the idea of the location of the valence and conduction band edges can be gathered from flat band potential [16]. The flat band potential is

obtained from the Mott-Schottky plot by extrapolation of the straight-line section to the zero capacitance and reading the intercept. The flat band potentials were -0.1 V and 0.2 V with respect to Ag/AgCl reference for the CZTS films annealed at 400°C and 500°C.

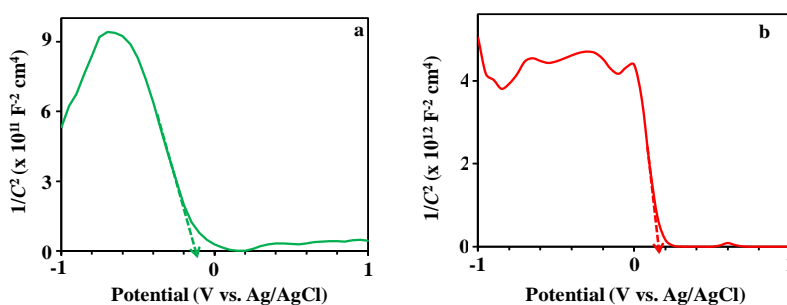


Fig. 6. Mott-Schottky plot for the samples annealed at different temperatures.

4. Conclusions

Copper, zinc, tin, and sulfur were electrodeposited together in a single-step on to a gold substrate using glycine. The characteristics of the deposits were found to alter with the annealing temperature. Agglomeration and crystallinity improved with annealing temperature. However, the loss of sulfur was more in sample annealed at 500°C. The growth of secondary phases increased at high-temperature annealing. CZTS deposit annealed at 400 °C showed a desirable composition ratio.

The optical characteristics of the deposits showed significant absorbance over all wavelengths for both the samples. The band gap of the particles did not change significantly with annealing temperature. Capacitance–potential studies showed the Mott-Schottky plot with a negative slope characteristic of p-type conductivity. The charge carrier concentration was estimated to range between 10^{11} and 10^{19} cm^{-3} . Current- voltage studies in the presence and absence of light source confirm that the thin-films are suitable for solar cell applications.

Acknowledgments

Authors would like to thank the Department of Science and Technology – Solar Energy Research Initiative (DST-SERI) for financing the research work under the Grant No. SEDST/TMC/SERI/2K12/57 and DST-SERB under the Grant No. SR/FTP/ETA-412/2013 for the analytical facilities.

References

- [1] V. Subramanian, Global Challenges in Energy and Environment- ICEE proceedings 2018; Single-step electrodeposition of CZTS thin film for solar cell application: Effect of annealing time, Springer, 1 (2019).
- [2] R. Manivnnan, S. N. Victoria, Sol. Energy **173**, 1144 (2018).
- [3] A. Paraye, R. Sani, R. Manivannan, S. N. Victoria, App. Surf. Sci. **435**, 1249 (2018).
- [4] W. Daranf, M. S. Aida, N. Attaf, J. Bougdira, H. Rinnet, J. Alloys and Compounds **542**, 22 (2012).
- [5] S. Swami, A. Kumar, V. Dutta, Energy Proceedia **33**, 198 (2013).
- [6] S. Tulshi, R. Dhyey, P. Malkeshkumar, M. Indrajit and R. Abhijit, Mater. Chem. Phys. **171**, 63 (2016).
- [7] S. M. Pawar, B. S. Pawar, A. V. Moholkar, D. S. Choi, J. H. Yun, J. H. Moon, S. S. Kolekar, J. H. Kim, Electrochimica Acta **55**, 4047 (2010).

- [8] C. P. Chan, H. Lam, C. Surya, Sol. Energy Materials and Solar Cells **94**, 2017 (2010).
- [9] R. Sani, R. Manivannan, S. N. Victoria, Chal. Lett. **14**, 165 (2017).
- [10] R. Sani, R. Manivannan, S. N. Victoria, J. Electrochem. Sci. Tech. **9**, 308 (2018).
- [11] K. V. Gaurav, J. H. Yun, S. M. Pawar, S. W. Shin, M. P. Suryawanshi, Y. K. Kim, G. L. Agawane, P. S. Patil, J. H. Kim, Mater. Lett. **108**, 316 (2013).
- [12] S. G. Lee, J. Kim, H. S. Woo, Y. Jo, A. I. Inamdar, S. M. Pawar, H. S. Kim, W. Jung, H. S. Im, Curr. Appl. Phys. **14**, 254 (2014)
- [13] J. J. Scragg, P. J. Dale, L. M. Peter, Electrochem. Comm. **10**, 639 (2008).
- [14] R. C. Alkire, D. M. Kolb, J. Lipkowski, P. N. Ross, Advances in electrochemical science and engineering- Photoelectrochemical Materials and Energy Conversion Processes, 12, Wiley-VCH, pp. 12.
- [15] Y. H. Khattak, F. Baig, H. Toura, I. Harabi, S. Beg, B. M. Soucase, App. Surf. Sci. **497**, 143794 (2019).
- [16] S. M. Camara, L. Wang, X. Zhang, Nanotechnology **24**, 495401 (2013).
- [17] A. N. Mallika, A. R. Reddy, K. V. Reddy, J. Adv Ceramics. **4**, 123 (2015).
- [18] X. Liu, K. Zhang, M. Li, Preparation and properties of Cu₂ZnSnS₄ nanoparticles by solvothermal method, Materials design processing and applications, Trans Tech Publications, Switzerland, 1668 (2013).
- [19] H. R. Jung, S. W. Shin, K. V. Gaurav, M. G. Gang, J. Y. Lee, J. H. Moon, J. H. Kim, Electron. Mater. Lett. **12**, 139 (2016).
- [20] N. P. Huse, A. S. Dive, K. P. Gattu, R. Sharma, Mater. Sci. Semicon. Processing **67**, 62 (2017).